Performance assessment of all-air heating in an office cubicle equipped with an active supply diffuser in a cold climate

Mehrdad Rabani[a, b, *]

Mehrdad.Rabani@oslomet.no

Habtamu Bayera Madessa[a]

Natasa Nord[b]

Peter Schild[a]

Mads Mysen[a]

[a]Department of Civil Engineering and Energy Technology, Oslo Metropolitan University, Norway

[b]Department of Energy and Process Engineering, Norwegian University of Science and Technology, Norway

*Corresponding author. Department of Civil Engineering and Energy Technology, Oslo Metropolitan University, Norway.

Abstract

Low-temperature space heating systems play a prominent role in improving the indoor air quality (IAQ) and thermal comfort of energy efficient buildings in cold-climate countries such as Norway. All-air heating (AAH) systems can be a practical solution because they simplify the space heating system and use low temperature energy sources. However, temperature stratification and deficient air distribution in the occupied part of the room can reduce the AAH performance. This study evaluated the performance of a low-temperature AAH system in an office cubicle designed in accordance with the Norwegian passive house (PH) standard and equipped with an active supply diffuser. Unlike conventional supply diffuser, active supply diffusers have variable slot opening permitting draught-free airflow adjustment with moving plates changing position, so that a constant supply air velocity was achieved. System performance simulations were validated by experimental data and then analysed for various supply and outdoor conditions using thermal comfort indices, IAQ indices, and the Archimedes number (Ar). The results showed that, when negatively buoyant air was supplied, the maximum indoor temperature difference between 0.1 m and 1.1 m above the floor was around 1.5K, which is within the recommended comfort range. Furthermore, the air diffusion performance index (ADPI) analysis showed a relatively high diffusion of air in the occupancy zone for all the scenarios, with the minimum ADPI around 75% for the scenarios with a negative Archimedes number. The active supply diffuser could satisfy the thermal comfort requirement even when the system was operating with the minimum airflow rate.

Keywords: All-air heating; Active supply diffuser; ADPI; Temperature stratification; Thermal comfort

Nomenclature

Roman symbols

A

heat surface area (m^2)

ACE

air change efficiency (–)

ACE_i

local air change efficiency at point i (–)

ACE_{avg}

average air change efficiency in the occupancy zone (—)

ACH

air change per hour (1/h)

ADPI

air diffusion performance index (—)

Ar

Archimedes number (—)

a_o

net opening area of active supply diffuser (m^2)

Cp

specific heat capacity (J/(kg.°C))

EDT

effective draught temperature (°C)

e_a^{21}

approximate relative error of the variable of interest (—)

Fcl

clothing area factor (—)

GCI

grid convergence index (—)

GCI_{fine}^{21}

fine-grid convergence index (—)

g

gravitational acceleration (m/s^2)

hc

convective heat transfer coefficient ($W/(m^2 \cdot K)$)

Icl

thermal clothing insulation (clo, 1clo = 0.154 (m^2·K/W))

L

thermal load on the body (W/m^2)

M

metabolic rate (met, $1\text{met} = 58\ \text{W/m}^2$)

N_i

grid numbers ($i = 1,2,3$)

P_a

partial pressure of water vapor (Pa)

PMV

predicted mean vote (—)

PPD

predicted percentage dissatisfied (—)

Q_{gain}

internal heat gains (W)

Q_{infil}

infiltration heat losses (W)

Q_{vent}

heat loss due to ventilation (W)

Q_{trans}

transmission heat loss (W)

r_{21}

grid refinement ratio (—)

T_a

air temperature in each region of control volume (°C)

$T_{ave.o}$

spatial average air temperature in the occupancy zone (°C)

T_i

local air temperature at point i (°C)

T_{out}

outdoor temperature (°C)

T_{in}

average indoor temperature (°C)

T_s

supply air temperature (°C)

T_e

exhaust air temperature (°C)

Tr

mean radiant temperature (°C)

Tcl

clothing surface temperature (°C)

U_{trans}

overall heat transfer coefficient (W/(m^2·K))

u_o

supply air velocity (m/s)

V

room gross volume (m^3)

$\dot{V}_s$

supply airflow rate (m^3/s)

v_i

local air velocity at point i (m/s)

W

active work (W)

w

characteristic length (m)

y+

dimensionless wall distance

Greek symbols

β

thermal expansion coefficient (1/K)

δ

apparent order (–)

δ δ_{ave}

ave average apparent order (–)

ρ_{air}

air density (m^3/kg)

$\varnothing_i$

variable of the interest (i = 1,2,3)

$\varnothing_{ext}^{21}$

extrapolated value of the variable of interest (–)

ε_T

temperature effectiveness (–)

τ_n

nominal time constant (s)

τ_i

local mean age of air at point i in the occupancy zone (s)

$< \overline{\tau} >$

average age of air in the occupancy zone (s)

1. Introduction

To improve energy security and sustainability and increase the use of renewable energy, the EU has set a target of reducing greenhouse gas emissions by at least 40% by 2030 as compared with 1990 [1]. Buildings consume a large portion of the total energy used and contribute about one-third of the total greenhouse gas emitted, so reducing building energy use is essential if this target is to be achieved.

Technically, substantial reductions in energy use and greenhouse gas emissions in the building sector can be achieved by retrofitting buildings to nearly zero energy level. In particular, reducing heat loss through higher insulation levels has been proposed as one of the most reliable and cost-effective methods of achieving the EU's ambitious goal, as demonstrated by the passive house (PH) concept. The heating demand of buildings designed in accordance with the PH standard is very low, e.g. 20 kWh/m^2·year for passive office buildings in Oslo, Norway [2], so the space heating demand could be covered by low-temperature heating systems such as ventilation radiators [3] and all-air heating (AAH) systems.

AAH generally means the supply of warm air at acceptably hygienic airflow rates, usually via a ventilation system that covers both ventilation and space heating demands. Mixing and displacement are the main principles of ventilation applied. Mixing ventilation features a high momentum of air supplied outside the zone of occupancy [4], while displacement ventilation is characterized by the supply of air at the floor level at very low velocity [5].

The main task of a ventilation system is to satisfy the indoor air quality (IAQ) requirements while, at the same time, providing a pleasant air velocity and uniform temperature distribution in the zone of occupancy. In this regard, the performance of AAH might sometimes be questioned, depending on the outdoor air condition, the supply air temperature and airflow rate, and the internal heat load. In one attempt in the 1970s, a simple form of room heating was tested using overheated temperature supply air at ceiling level. The aim was to avoid the need for local space heating installations in the form of radiators. Unfortunately, the result was a significant degree of temperature stratification and poor IAQ in the occupancy zone, because the space heating demands in the 1970s were considerably higher than for modern passive houses [6].

Afterwards, several authors [7–13] have investigated the performance of conventional AAH systems. Fisk et al. [7] carried out several experiments to measure the ventilation effectiveness in a laboratory chamber with a ceiling supply/exhaust configuration. The results indicated that when a variable air volume (VAV) system is used with heated air supplied at a minimum airflow rate, the ventilation effectiveness varies from 69% to 89%, and significant short-circuiting of ventilation air between the supply air diffuser and return air is observed.

Offermann and Int-Hout [8] measured ventilation effectiveness in an office building heated using various supply and return positions. They found that when the supply and exhaust are located at ceiling level, a ventilation effectiveness of 73% is obtained when the room average temperature is 8 °C lower than the supply air temperature. They also observed short-circuiting of airflow from the supply to exhaust.

Novoselac and Srebric [9] simulated IAQ in five typical indoor spaces with various ventilation and heating strategies, including a personal office with an AAH system. Their results showed that a recirculation zone at floor level created a considerable stratification of contaminants in the lower part of the occupancy zone. Liu and Novoselac [10] also found that the main challenge in applying AAH is poor air distribution, because vertical temperature stratification leads to poor IAQ and thermal discomfort.

Olesen et al. [11] experimentally studied the air distribution and ventilation effectiveness of various heating/cooling and ventilation strategies. They found that in all strategies adopting warm air heating, a warm air layer is formed near the ceiling and the ventilation effectiveness can be as low as 40%. Consequently, an increased amount of ventilation is required.

Krajčík et al. [12] experimentally analysed the ventilation effectiveness and air distribution in a test room located in a low-energy building equipped with AAH and a floor heating system. Their results, in the case of using AAH, did not support a significant risk of thermal discomfort due to temperature stratification, but they did find that a stale air region in the occupancy zone of the room was generated with a uniform low temperature leading to a low ventilation effectiveness.

Risberg et al. [13] carried out several Computational Fluid Dynamics (CFD) simulations on the performance of three different heating systems (floor heating, air-air heat pump, and AAH) in a multi-zone low-energy residential building in northern Sweden. The results indicated that AAH cannot create uniform velocity and temperature distributions. A more functional AAH system would need much improved performance.

Using active supply diffusers at ceiling level seems to be an interesting solution for AAH systems. As a part of a retrofitting strategy, existing constant air volume (CAV) systems can be converted to VAV systems using active supply diffusers. However, a comprehensive assessment would be needed to find out if it is a robust alternative solution for space heating, especially in a cold climate. Therefore, the aim of this study was to evaluate the performance of a low-temperature AAH system in an office cubicle designed in accordance with the Norwegian PH standard and equipped with an active supply diffuser.

The rest of the paper is organized as follows. Section 2 will introduce various indices commonly used in the evaluation of the performance of a building ventilation system and occupant thermal comfort. Applying different indices can provide interesting information about the performance of active supply diffuser in terms of temperature stratification, occurrence of short-circuiting, ventilation air exchange efficiency, and air diffusion uniformity in the zone of occupancy, as well as useful information about occupant satisfaction with the indoor thermal environment. It should be mentioned that the details of the equations describing each index are provided in the Appendix.

The first part of Section 3 will describe the case study and how the corresponding CFD model was simplified and generated to replicate the experimental case. Furthermore, the CFD details selected for the simulations and the validation of the numerical method will be given. The second part of Section 3 will explain the choice of the main parameters defining the scenarios and how the indices were calculated and implemented for the case study. The last section of the paper will present the results obtained from simulations and discuss and interpret the AAH system performance in terms of the various indices.

2. Theoretical background

To evaluate the performance of ventilation system in terms of improving IAQ and thermal comfort, indices and a dimensionless parameter have been defined as follows:

2.1. Predicted mean vote (PMV) and predicted percentage dissatisfied (PPD)

PMV is an index frequently used in thermal comfort analysis. It evaluates the thermal sensation of the occupants based on a seven-point scale (from −3, cold, to 3, hot) by taking air temperature, mean radiant temperature, air velocity, air humidity, metabolic rate, and clothing insulation level into consideration [14]. PPD provides a quantitative prediction of thermal dissatisfaction based on the seven-point scale. A desirable thermal environment for a PH office building is one that satisfies the following criteria: PPD <10%, associated with $-0.5 < PMV < 0.5$, according to comfort category II, which is the level of expectation for new and retrofitted buildings [15].

2.2. Air diffusion performance index (ADPI)

ADPI is a widely applied design index that quantifies the performance of diffusers based on their creation of spatial uniformity in air velocity and temperature and its contribution to thermal comfort [16]. It is defined as the percentage of measurement locations where the criteria for Effective Draught Temperature (EDT) and air velocity are met (for further details, see the Appendix) [17]. A good ventilation system should generate an ADPI higher than

80%, i.e. at least 80% of the points considered in the space investigated meet the criteria [18].

2.3. Air change efficiency (ACE)

Ventilation effectiveness shows how well the system can remove contaminants from a room. ACE is often regarded as an index of ventilation effectiveness because it indicates how efficiently the supply air is distributed throughout the occupancy zone [19]. ACE of a room in an ideal mixing ventilation system with fully mixed model is 50%. A system with ACE higher than 50% can result in energy saving by reducing the minimum supply airflow rate required to maintain an acceptable IAQ level. In contrast, a system with ACE lower than 50% would lead to higher energy use due to the increase in supply airflow rate required to satisfy the IAQ requirements [20].

2.4. Temperature effectiveness

Temperature effectiveness (ε_T) is analogous to the concept of ventilation effectiveness in removing contaminants, where the concentration is replaced by the temperature [21]. A desirable ventilation system should generate $\varepsilon_T > 1$, indicating a small temperature difference between the supply and the occupancy zone. Moreover, this implies that the supply temperature can be lowered in heating mode. Conversely, a ventilation system with $\varepsilon_T < 1$ means that the supply temperature must be increased to fulfil the temperature requirements in the occupancy zone [21].

For the four above introduced indices, mathematical expressions are given in Appendix.

Analysing ventilation system performance using indices is generally accompanied by introducing dimensionless parameters that describe various characteristics of the supply air jet and room airflow. One of the most useful dimensionless parameters when assessing ventilation system performance is Archimedes number (Ar) [21]. This determines the amount of circulation in the room and compares the strength of buoyancy force in the room with the momentum of the supply air, and is defined in Eq. (1) [22].

$$\mathrm{Ar} = \frac{g\beta w\left(T_e - T_s\right)}{u_o^2} \tag{1}$$

where the T_s (°C) is the supply air temperature, T_e (°C) is the exhaust air temperature, u_o (m/s) is the supply air velocity, w (m) is the characteristic length, g (m/s^2) is the gravitational acceleration, and β (1/K) is the coefficient of thermal expansion. The characteristic length can be defined as the square root of the supply area in the case of a diffuser (in mixing ventilation) or the height of the supply in the case of slot opening (in displacement ventilation). In this study, in order to facilitate the interpretation of results, Eq. (1) was reformulated as in Eq. (2):

$$\mathrm{Ar} = \frac{g\beta a_o^{\frac{5}{2}}\left(T_e - T_s\right)}{\dot{V}_s^2} \tag{2}$$

where a_o (m^2) is the net opening area of the active supply diffuser and $\dot{V}_s$ (m^3/s) is the airflow rate.

Although there have been relatively extensive studies on the performance of mixing ventilation systems in cooling mode [17,23–25], only a few studies [9,10,26] have investigated the connection between the ventilation system performance factors and the air supply jet parameters in heating mode. The importance of heating mode is shown by the fact that it is not usually so easy to achieve favourable mixing in heating mode as in cooling mode. The main objective of this study therefore was to examine the performance of a mixing ventilation system equipped with a radial active supply diffuser with adjustable slot openings for the space heating of an office cubicle designed in accordance with the Norwegian PH standard. In other words, the aim was to investigate the potential of applying a low-temperature heating system equipped with an active supply diffuser. In doing this, we determined the impact of various supply airflow rates and temperatures and various outdoor conditions on the AAH performance in terms of IAQ and air distribution effectiveness using the dimensionless Archimedes number.

3. Methodology

We used computational fluid dynamics (CFD) to simulate AAH with mixing ventilation, and then analysed the resulting air temperature and velocity distributions and the above-mentioned indices in the office room. The suitability of CFD in simulation of such applications has long been accepted [27].

The following sections elaborate the details of 1) the case study and CFD model definition, and 2) the definition of the scenarios and the implementation of the indices.

3.1. Case study and CFD model definition

3.1.1. CFD software, geometry and boundary conditions

The simulations were carried out using the commercial CFD software Star-CCM+. The case study was a standard office cubicle constructed in accordance with the Norwegian PH standards [28] and located in Oslo, Norway. Fig. 1(a) illustrates the computational domain comprising an office cubicle measuring 4.2 m × 2.25 m × 2.7 m, with one window measuring 1.7 m × 2.0 m. A seated occupant was modelled using a cylinder 1.1 m high and 0.6 m in diameter. In addition, a PC, table, and lighting fixture were modelled using three rectangular cubes measuring 0.3 m × 0.3 m × 0.4 m, 2 m × 0.8 m × 0.02 m, and 1.2 m × 0.18 m × 0.04 m, respectively. It should be noted that, compared to the experimental configuration (Fig. 1(b)) [28], the table and PC were simplified to facilitate the simulations.

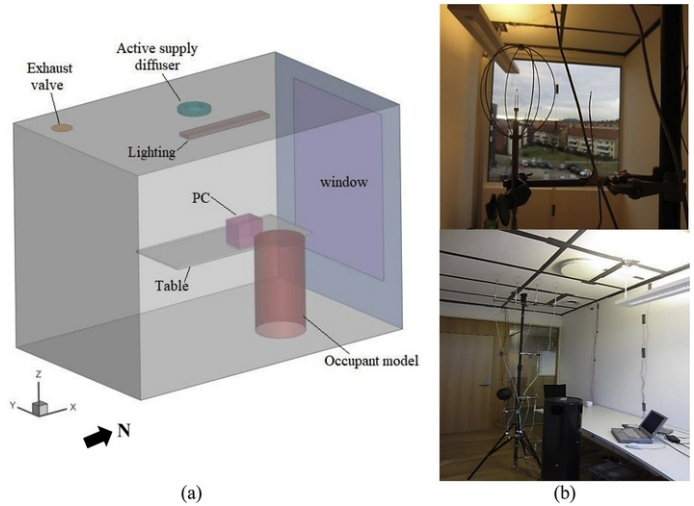

Fig. 1. (a) CFD model of the office cubicle (b) experimental configuration for the office cubicle [28].

alt-text: Fig. 1

A radial active supply diffuser in the ceiling was simulated. The diffuser model shown in Fig. 2(a) was a TTC-250 active supply air diffuser used for demand control of airflow rate by means of controllable slot openings. It is designed for the lowest possible energy usage without imperilling comfort requirements. Unlike typical VAV systems, in which the supply air velocity changes as the airflow rate varies due to the constant supply area, the variable slot openings in the active supply diffuser (see Fig. 2(b)) can maintain a constant supply velocity to ensure a draught-free performance for varying airflow rates [29]. It should be noted that only the part of the sleeve coupling module of the active diffuser projecting below the false ceiling was modelled in this study. In addition, the exhaust valve was modelled using a simple round outlet with a diameter of 0.25 m.

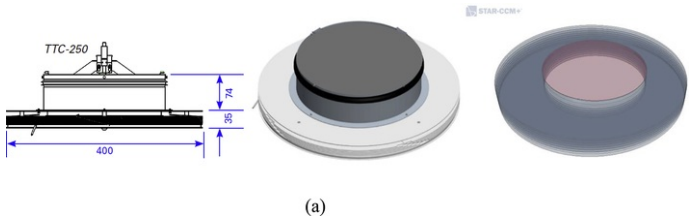

Fig. 2a. Active supply diffuser dimensions (left), the configuration (middle) [29], and the active diffuser modelled in Star-CCM+ (right).

alt-text: Fig. 2a

Fig. 2b. Adjustment of slot openings in the active supply diffuser [29].

alt-text: Fig. 2b

The boundary conditions of the CFD model were defined as follows:

- **Inlet:** A uniform velocity profile was specified at the inlet of the active diffuser for the simulation. It should be noted that since the inlet was in the ceiling (the red circle in Fig. 2(a)), the inlet velocity was modified according to the selected airflow rates for various scenarios under consideration. Furthermore, the slot openings of the diffuser were adjusted according to the airflow rate in different cases so that the supply air velocity remained constant at the outlet of slot openings. The amount of air was selected to provide the minimum airflow rate required by the Norwegian PH standard for offices [30]. The supply temperature was also changed in different scenarios. The details of these supply condition calculations are explained in section 3.2. ~~Scenarios, parameters, and indices implementation.~~
- **Outlet:** At the outlet, zero gauge-pressure was defined as the boundary condition.
- **Occupant, lighting and equipment:** The occupant, lighting and PC were modelled as heat sources generating a constant rate of heat transfer. The heat emitted by the occupant, the lighting, and the PC was 120 W, 136 W, and 30 W, respectively [28]. Adiabatic boundary conditions were applied for the table.
- **Floor, side walls, and window:** To be able to apply boundary conditions for the various parts of the envelope, the following U_{trans} values were chosen based on the experimental conditions [28]: 0.14 W/(m^2·K) for the external wall, 0.25 W/(m^2·K) for the internal walls, 0.78 W/(m^2·K) for the window, 0.10 W/(m^2·K) for the roof, and 0.07 W/(m^2·K) for the floor. These experimental conditions were provided to satisfy the Norwegian PH standard. From these, the transmission losses Q_{trans} (W) through the envelope were calculated using Eq. (3), and the value Q_{trans}/A (W/m^2) for each part of the envelope was used as the heat flux boundary condition in the software.

To maintain the desired average air temperature, based on the thermal comfort requirements for comfort category II [15], the air temperature supplied by the active diffuser was adjusted in accordance with the calculations from the energy balance equations (Eqs. (3)–(6)). Infiltration losses, Q_{infil} (W), represents the heat loss due to infiltration caused by a pressure difference between indoor and environmental conditions. An air change per hour (ACH) of 0.23 for the infiltration was used for the calculation of infiltration losses based on the experimental conditions [28].

$$Q_{trans} = U_{trans} \cdot A \cdot \left(T_{in} - T_{out}\right) \quad \textbf{(3)}$$

$$Q_{gain} - \left(\sum Q_{trans} + Q_{infil}\right) = Q_{vent} \quad \textbf{(4)}$$

$$Q_{vent} = \rho_{air} \dot{V}_s C_p \left(T_{in} - T_s\right) \quad \textbf{(5)}$$

$$Q_{infil} = \rho_{air} \frac{ACH.\ V}{3600} C_p \left(T_{in} - T_{out}\right) \quad \textbf{(6)}$$

where Q_{gain} (W) is the internal heat gain, Q_{vent} (W) is the heat loss due to ventilation, T_{in} (°C) is the average indoor temperature, $\dot{V}_s$ (m^3/s) is the supply airflow rate, and V (m^3) is the gross volume of the room.

3.1.2. Mesh study

In accordance with the geometry modelled, the associated mesh domain was generated in the Star-CCM + software. The unstructured polyhedral-shaped mesh was taken into account in the computational domain. It is numerically more stable and more precise than a comparable tetrahedral mesh, and fewer polyhedral cells are needed to achieve a specified accuracy than even Cartesian hexahedral cells [31]. The cell sizes in the proximity of the solid surfaces as well as the supply and exhaust were refined to accurately simulate the convective heat transfer due to the buoyancy force of the heat source plumes and to precisely capture the characteristics of the supply jet. The refinement procedure was carried out using a surface remesher and prism

layer mesher to modify the cell quality.

Since the common purpose of simulations of indoor climate problems is to achieve a grid independent solution [32], grid convergence indexing was used in this study [33]. In this method, three grid numbers $N_3 21$ are usually required to obtain a grid convergence index (GCI) ensuring convergence to the extrapolated value [33]. The GCI, therefore, was calculated as follows:

$$GCI_{fine}^{21} = \frac{1.25\, e_a^{21}}{r_{21}^{\delta} - 1} \quad \textbf{(7)}$$

where GCI_{fine}^{21} is the fine-grid convergence, e_a^{21} is the approximate relative error of the variable of interest (velocity in this study, Eq. (8)), r_{21} is the grid refinement ratio (considered constant in this study, see Eq. (9)), δ is the apparent order given in Eqs. (10), and 1.25 is the safety factor for comparing three or more grids.

$$e_a^{21} = \left| \frac{\emptyset_1 - \emptyset_2}{\emptyset_1} \right| \quad \textbf{(8)}$$

$$r_{21} = \left(\frac{N_1}{N_2} \right)^{\frac{1}{3}} \quad \textbf{(9)}$$

$$\delta = \frac{1}{\ln(r_{21})} \left| \ln \left| \frac{\emptyset_3 - \emptyset_2}{\emptyset_2 - \emptyset_1} \right| + q(\delta) \right|, \; (q(\delta) = 0 \text{ for constant r}) \quad \textbf{(10)}$$

where $\varnothing_{1,2,3}$ is the variable of interest for grid numbers N_1, N_2, and N_3, respectively, in the grid convergence analysis.

The extrapolated value was also calculated as follows:

$$\emptyset_{ext}^{21} = \left(\frac{r_{21}^{\delta} \emptyset_1 - \emptyset_2}{r_{21}^{\delta} - 1} \right) \quad \textbf{(11)}$$

To ensure that the grids were in the asymptotic range of convergence, the following expression in Eq. (12) was checked by:

$$\frac{GCI_{32}}{r^{\delta} GCI_{21}} \cong 1 \quad \textbf{(12)}$$

Three grids with $N_3 = 358475$, $N_2 = 1215920$, and $N_1 = 4132521$ with the grid refinement ratio $r = 1.5$ were considered for the grid independence study. Table 1 illustrates the calculation of GCI for the three grid numbers. It should be noted that the supply air temperature, airflow rate, and the outdoor temperature in this case were set to 24.1 °C, 49.4 l/s, and −1.8 °C respectively, in accordance with the experimental conditions.

Table 1 Calculation details of discretization error and GCI.

alt-text: Table 1

	Grid N_1	Grid N_2	Grid N_3
Cell number	4132521	1215920	358475
$\delta_{ave.}$	1.944425		
GCI (%)	$GCI_{21} = 0.15137$	$GCI_{32} = 0.364798$	N/A
r	1.5	1.5	N/A
$\frac{GCI_{32}}{r^{\delta} GCI_{21}} \cong 1.095509$			

The variable of interest was the air velocity along the vertical line from height 0.1 m–1.8 m above the floor in the occupancy zone. The dimensions of the occupancy zone are shown in Fig. 3(a) [34]. The values of $\delta_{ave.}$ and GCI in Table 1 are the average of the local values along the measurement line shown in Fig. 3(a). As Table 1 shows, the solution was in the asymptotic range of convergence. To investigate the grid convergence qualitatively, the velocity variation along the measurement line (Fig.

3(a)) for the three grids was compared with the extrapolated values (obtained from Eq. (11)), as shown in Fig. 3(b).

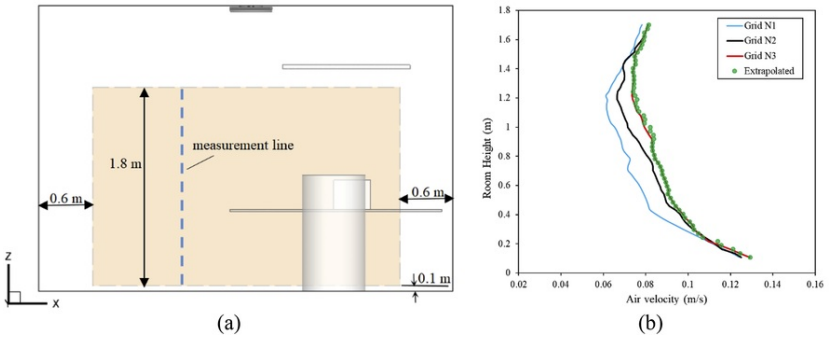

Fig. 3. (a) Schematic of the occupancy zone dimensions [34] and the location of the measurement line in the occupancy zone, (b) Velocity variation along the measurement line for different grid numbers (at cross section Y = 1.4 m).

alt-text: Fig. 3

It can be seen that the finest grid, the red line in Fig. 3(b), roughly followed the extrapolated values. The y + frequency for this case is illustrated in Fig. 4(a) near the walls. The $y^+ \sim 0.15$ with a high cell number frequency occurred for all the surfaces. However, some higher y^+ frequencies were observed around the supply diffuser, but still with $y^+ < 5$ [35] indicating the mesh was properly refined in this critical region to maintain the supply jet characteristics (Fig. 4(b)).

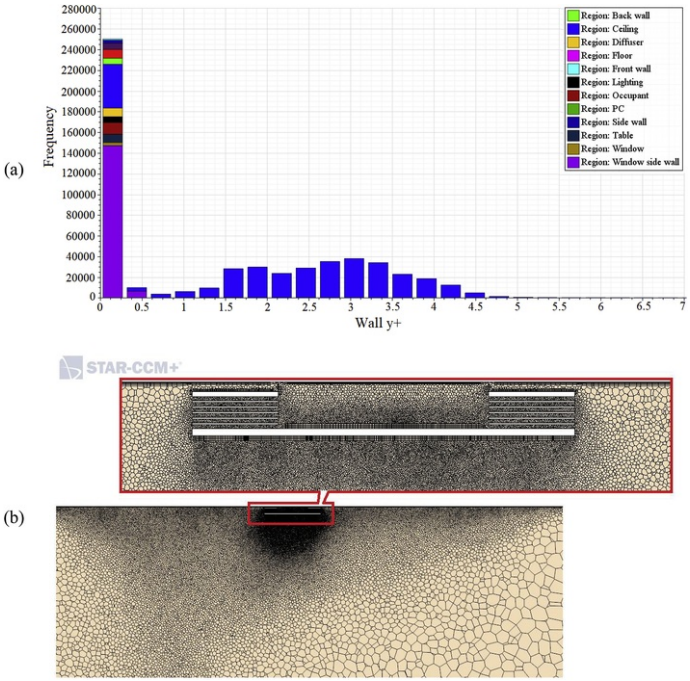

Fig. 4. (a) y^+ frequency near the walls, (b) Mesh quality around the active supply diffuser.

alt-text: Fig. 4

3.1.3. Discretization method, solver, and turbulence model

The Reynolds-Averaged Navier-Stokes (RANS) equations were discretized by means of the finite volume method (FVM) and were solved along with the energy equation using the segregated solver in the steady state condition. The segregated

solver applied the SIMPLE pressure-velocity coupling algorithm where the mass conservation constraint on the velocity field was fulfilled by solving a pressure-correction equation. In addition, the surface-to-surface (S2S) model was applied to model the radiation heat transfer in the room, treating the air as transparent to radiation. Furthermore, the emissivity of all the walls was considered equal to 1 because the materials typically used in an office usually have an emissivity around 1 [36]. The emissivity of the window glazing was 0.84 [37].

The flow regime was considered fully turbulent. As Hoof et al. [38] suggested, the turbulence model can strongly affect the results and the validation of numerical results should be performed using experimental data to ensure the reliability of the numerical method. We therefore investigated four different turbulence models of *Standard k–ω*, *Shear Stress Transport (SST) k–ω*, *Standard k–ε*, and *Realizable k–ε* and the results were compared with the experimental data [28] to identify which turbulence model could best replicate the experimental velocity and temperature trends. The dimensions, properties, and geometry of various components of the experimental configuration have been described in detail in Section 3.1.1. Furthermore, the details of the experimental setup and the location of the air temperature and velocity sensors are shown in Table 2 and Fig. 5, respectively. It should be noted that the cylinder is shown with a dashed line because the cross section did not include the cylinder.

Table 2 Experimental parameters used in the validation of numerical model.

alt-text: Table 2

Parameter	Value
Supply airflow rate (l/s)	49.4
Supply temperature (°C)	24
Outdoor temperature (°C)	−1.8
Total opening height in the active supply diffuser (m)	0.026
Internal heat gains (W)	Occupant: 120 Lighting: 136 PC: 30

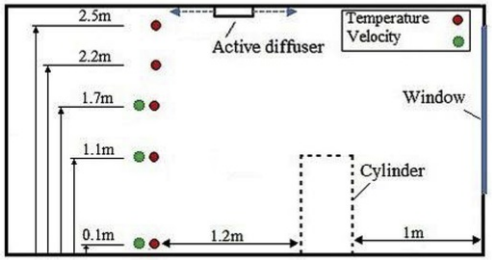

Fig. 5. Schematic of the position of the air temperature and air velocity sensors used in the experimental validation of the model at Y = 1.4 m

alt-text: Fig. 5

Fig. 6(a) shows the comparison of air velocity variation along the measurement line (Fig. 3(a)). The results in Fig. 6 (a) show that the *Standard k–ε* model predicted the air velocity variation closer to the experimental data (within the uncertainty range) than the other turbulence models. Although all four turbulence models predicted the temperature variation Fig. 6(b)) in almost the same manner. We therefore selected the *Standard k–ε* turbulence model for the simulations in this study.

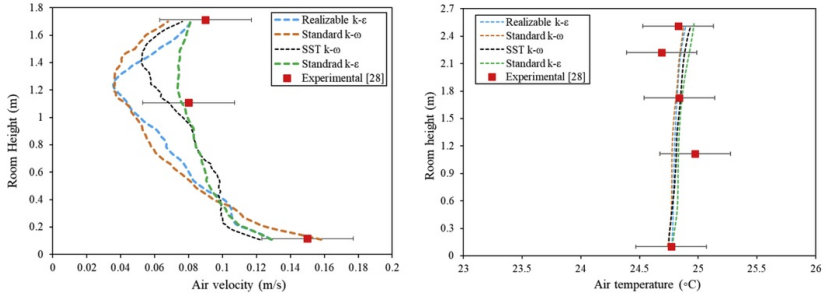

Fig. 6. (a) Air velocity and (b) air temperature variations along the measurement line for the four turbulence models.

alt-text: Fig. 6

The steady state condition was reached by checking the mass flow rate difference between the exhaust and supply terminals as well as by monitoring the exhaust temperature during the simulations. The simulations were therefore stopped when the mass imbalance was approximately zero and the exhaust temperature remained unchanged.

3.2. Scenarios, parameters, and indices implementation

In this study, to define various scenarios, the supply air temperature was adjusted to compensate for the transmission and infiltration heat losses and to maintain the average indoor air temperature desired according to the thermal comfort requirements for comfort category II. Four different outdoor temperatures with four corresponding air supply temperatures at three different airflow rates were therefore considered for simulations, giving a total of twelve scenarios for analysis. The lowest outdoor temperature of −20 °C was selected based on the design outdoor temperature for Oslo, Norway, in the winter season [39]. The minimum airflow rate was chosen as the minimum airflow rate required in the Norwegian PH standard and the maximum airflow rate considered was the maximum airflow rate under which the TTC-250 active supply diffuser could operate. Table 3 describes the parameters and supply air conditions in the scenarios analysed.

Table 3 The main parameters for the scenarios investigated in this study.

alt-text: Table 3

Scenario	T_{out} (∘C)	T_s (∘C)	$\dot{V}_s$ (l/s)	Ar
S1	−20	24.8	49.4	-1.56×10^{-3}
S2	−15	24.2	49.4	-6.14×10^{-5}
S3	−7	23.2	49.4	2.22×10^{-3}
S4	−1.8	22.6	49.4	3.71×10^{-3}
S5	−20	26.4	16	-1.73×10^{-3}
S6	−15	24.6	16	-1.18×10^{-4}
S7	−7	21.6	16	2.57×10^{-3}
S8	−1.8	19.7	16	4.48×10^{-3}
S9	−20	25.5	26	-1.60×10^{-3}
S10	−15	24.3	26	-6.89×10^{-5}
S11	−7	22.5	26	2.34×10^{-3}

S12	−1.8	21.3	26	3.97×10^{-3}

It should be noted that in Table 3 $Ar > 0$ (scenarios S3, S4, S7, S8, S11, and S12) implies the AAH system is in "ventilation mode" and $Ar < 0$ (scenarios S1, S2, S5, S6, S9, and S10) implies "ventilation and heating mode". In other words, "ventilation mode" describes the performance of the system with a supply of positively buoyant air, where internal heat gains cover almost the whole space heating demand, while the "ventilation and heating mode" describes the performance of the system with a supply of negatively buoyant air, where the ventilation air performs the space heating task as well.

All the scenarios were evaluated using the four different indices, PMV/PPD, ADPI, ACE, and ε_T in terms of Archimedes number, to find out the integrated effects of various supply and outdoor conditions on the IAQ and thermal comfort. These indices were introduced in Section 2 and are described in detail in the Appendix.

In calculating the PMV and PPD, the mean radiant temperature and room average air temperature were generally very similar and using the latter value instead of the mean radiant temperature does not have a substantial effect on comfort calculations [40]. In an office building, moreover, the metabolic rate and clothing level of occupants commonly vary from 1 met. to 1.3 met. and 0.5 clo (in summer) to 1 clo (in winter), respectively [41–43]. These assumptions were therefore taken into account along with considering an indoor relative humidity of 50%, which is a typical value for commercial buildings all year round. The spatial air temperature and velocity distributions were obtained in Star-CCM+, and the post-processing to extract the PMV and PPD distribution was performed in MATLAB.

The ADPI was implemented using the method defined in ASHRAE standard 113 [17]. The air velocity and air temperature were therefore measured at various locations and heights in the zone of occupancy. Test point locations were distributed uniformly in the occupancy zone with horizontal spacing of 0.6 m with four measurement points at heights of 0.1, 0.6, 1.1, and 1.7 m above the floor, 48 points in total. Afterwards, Eq. (18), see Appendix, was applied to evaluate the performance of air diffusion.

In addition, to examine the ACE for various scenarios, the mean age of the air was measured using the passive scalar model definition. This implied attaching a virtual clock to each volume element of air. These virtual clocks were used to measure the age of the air in the room and Eq. (19), see Appendix, was then used to calculate the ACE in the room.

4. Results and discussion

This section has been divided into five subsections in order to analyse the performance of the active supply diffuser in terms of temperature stratification, air distribution, and thermal comfort indices as thoroughly as possible.

4.1. Air velocity distribution pattern and air temperature stratification in the room with an active supply diffuser

Fig. 7 shows patterns of airflow distribution near the active supply diffuser in the various scenarios. It was observed that adjusting the slot openings of the active diffuser could preserve the jet throw length almost all the way to the internal wall (opposite the window) in all the scenarios. However, very different distribution patterns were created in the window side of the room due to interference from the cold current from the window on the warm supply jet. In ventilation and heating mode with $Ar < 0$, the top two rows in Fig. 7, the jet was deflected downwards and buoyancy forces then opposed the warm flow leading the jet airflow to turn upwards and form a circulating region near the supply diffuser. The jet flow penetrated to the lowest height in scenario S6 because the Archimedes number was lower than in the other scenarios with $Ar < 0$. In ventilation mode with $Ar > 0$, the bottom two rows in Fig. 7, the supply jet was potentially unstable in the sense that the buoyancy forces worked to deflect the flow downwards. This effect was strongest in scenario S8 where the Archimedes number was higher than in the other scenarios, causing the supply jet to detach from the ceiling and drop a short distance from the supply terminal, resulting in the formation of a strong vortex in the interaction area with turbulent eddies in the supply jet and the surrounding air. It is worth noting that the cross section $Y = 1.4$ m was chosen to illustrate the results in order to properly capture both the airflow trace supplied by the active supply diffuser and its interaction with the cold airflow current from the window. In addition, the cross section also included the occupancy zone and the experimental points used for the validation of the model.

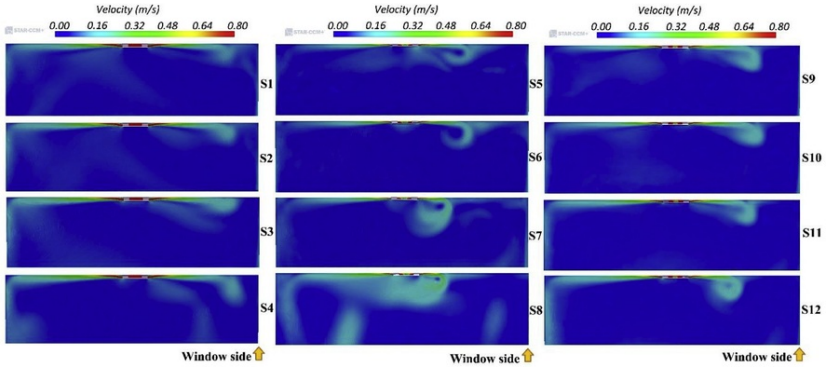

Fig. 7. Air velocity distribution in the room with the active supply diffuser for the various scenarios in a plane passing through the window (Y = 1.4 m).

alt-text: Fig. 7

Fig. 8 shows the vertical temperature variation along the measurement line extended beyond the zone of occupancy shown in Fig. 3(a). In general, the stratification in the scenarios with Ar < 0 (scenarios S1, S2, S5, S6, S9, and S10) was greater than in the other scenarios due to the supply of negatively buoyant air. However, the temperature stratification was not great. The maximum temperature difference between the ankle (0.1 m) and the seated head level (1.1 m) was approximately 1.5K, in scenarios S1, S5, and S9, which is still within the recommended range for the IAQ category II according to the standard EN ISO 7730 [15].

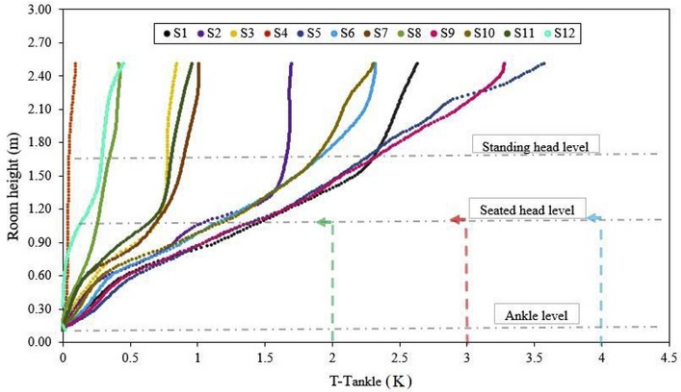

Fig. 8. Vertical temperature difference along the measurement line.

alt-text: Fig. 8

4.2. ADPI variation in the various scenarios

To evaluate the performance of the active supply diffuser in terms of diffusion and uniformity of air in the occupancy zone, we examined the ADPI index in the various scenarios. Fig. 9 (a) shows the location of 48 sampling points chosen to evaluate the ADPI index.

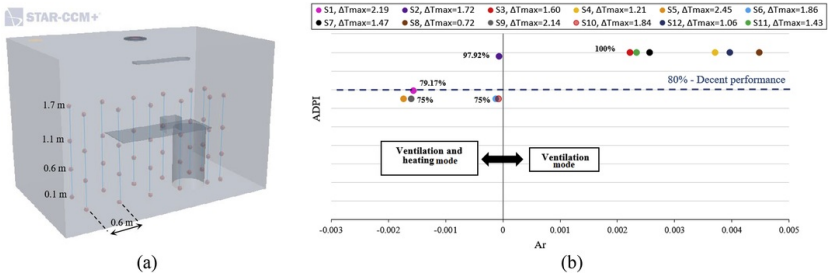

Fig. 9. (a) Position of sampling points, (b) ADPI variation in different scenarios.

alt-text: Fig. 9

In all the scenarios, see Fig. 9(b), the system showed acceptable performance, especially in ventilation mode, where $Ar > 0$. In ventilation and heating mode, however, system efficiency dropped slightly, though close to the good performance of ADPI = 80%. This is where the lowest ADPI percentages (around 75%) occurred, in scenarios S5, S6, S9, and S10. Furthermore, the maximum temperature difference between the ankle and seated head level was around 2.45 K, which was still below the ADPI maximum limit of 3K (see Appendix), and the maximum air velocity at the sampling points was always less than 0.35 m/s in all scenarios. It is worth mentioning that, in scenarios S5 and S6, in spite of supplying highly negative buoyant air at the minimum possible airflow rate, the active supply diffuser could create satisfactory performance in terms of a uniform diffusion of air in the occupancy zone.

4.3. ACE analysis in the occupancy zone

Fig. 10 presents the average ACE in the occupancy zone for the scenarios analysed along with the associated dispersion of ACE in each scenario reflected as error bars. The highest ACE of around 43% was obtained for scenarios S4 and S8 due to their high Archimedes number. The lowest ACE of around 27% was obtained in scenarios S5 and S9, where the Archimedes number was negative. In fact, high ACE values were always observed in the scenarios operating in ventilation mode and low ACE values were detected in ventilation and heating mode. The reason for this might be that in the ventilation mode, the supply of positively buoyant air assisted air movement in the room, while the negatively buoyant supply jet in ventilation and heating mode relatively obstructed the air from flowing into the occupancy zone and properly exchanging the room air. Although AAH systems often generate stagnant air in the occupancy zone leading the ACE to drop considerably, while relatively uniform temperature in the occupancy zone results in acceptable ADPI, the adjustment of slot openings in the active supply diffuser may have somehow remedied this problem.

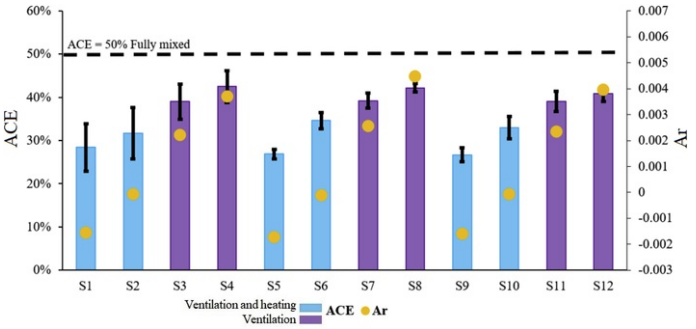

Fig. 10. Variation of average ACE in the occupancy zone.

alt-text: Fig. 10

With regard to ACE dispersion, indicated by the length of the error bars magnitude, this is the variation of the ACE in the room, indicating how well the air was distributed and exchanged in the occupancy zone. A large dispersion of ACE was found in scenarios S1-S4, where the active supply diffuser was operating with the maximum possible airflow rate, especially scenarios S1 and S2. This implies that the local mean age of air varied to some extent in different parts of the occupancy zone. The spatial distribution of local ACE in the room and the occupancy zone for these scenarios was therefore further investigated, as illustrated in Fig. 11. In ventilation and heating mode (scenarios S1 and S2), there was some evidence of stagnant air in the lower part of the occupancy zone, indicating relatively less contribution by the supply air to the air mixing in this part of the occupancy zone, while in the upper part of the occupancy zone, the room air was replaced faster by the supplied fresh air. However, the rather high ADPI seen in the previous section for scenarios S1 and S2 was due to the influence of buoyancy forces resulting from of

internal heat sources and the exchange of heat by thermal radiation. In ventilation mode (scenarios S3 and S4), a larger part of the occupancy zone experienced a good distribution of the fresh air. This can explain the higher variation in ACE in the scenarios S1 and S2 than in scenarios S3 and S4.

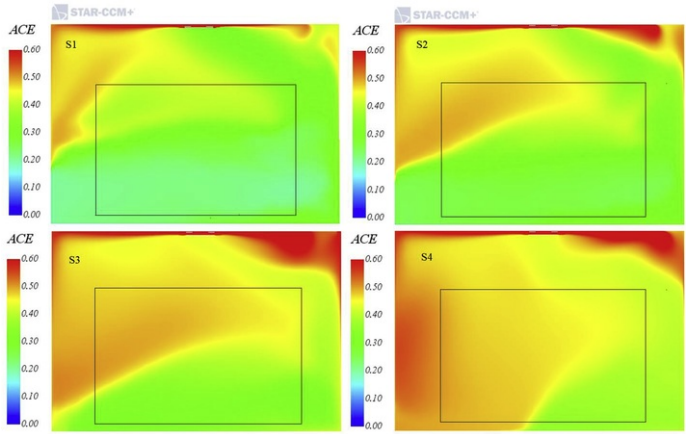

Fig. 11. Spatial distribution of ACE in the cross plane passing the window (Y = 1.4 m). Note: the black rectangle represents the occupancy zone.

alt-text: Fig. 11

4.4. Temperature effectiveness evaluation

The indoor thermal environment for the different scenarios was also evaluated using the temperature effectiveness index, ε_T, as shown in Fig. 12. Introducing negatively buoyant air to the test room resulted in low temperature effectiveness in the occupancy zone for the ventilation and heating mode scenarios (S1, S2, S5, S6, S9, and S10). This means that the average temperature in the occupancy zone was lower than in the exhaust and some of the supplied air circulated in the upper part of the room, reflecting a somewhat short-circuited airflow above the occupancy zone. However, using the active supply diffuser meant that, there was no pronounced difference between the scenarios in which the maximum (scenarios S1 and S2) and the minimum (scenarios S5 and S6) airflow rates were supplied. In ventilation mode, where the Archimedes number was positive, the temperature effectiveness reached as high as 1.17 and, as shown in Fig. 8, no sign of temperature stratification appeared.

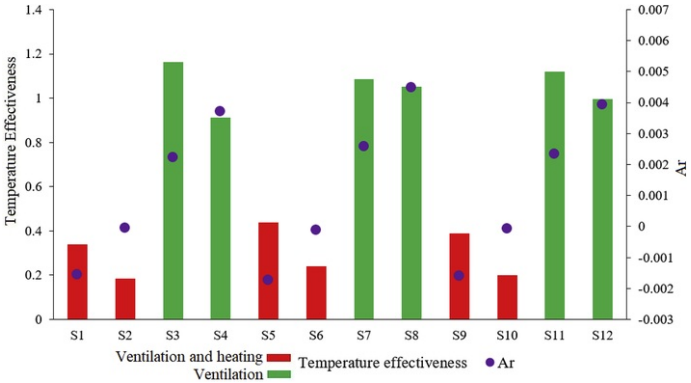

Fig. 12. Variation of temperature effectiveness, ε_T, in different scenarios.

alt-text: Fig. 12

Furthermore, if Figs. 10 and 12 are compared, different trends may be noted in the variation of ACE and temperature effectiveness as the Archimedes number changes. Both temperature effectiveness and ACE depend on the location of the supply and exhaust diffusers, the supply of positively or negatively buoyant air, and the ventilation airflow rate. Moreover, both the passive scalar (the indicator parameter introduced to calculate the age of air and ACE)

and the temperature (the indicator parameter in the temperature effectiveness calculation) are transported by convection and diffusion. However, the air temperature field is also influenced by radiation. This phenomenon results in a coupling between the convection, diffusion, and radiation heat transfer processes at room surfaces, which affects only the air temperature field, not the passive scalar distribution. As a result, a different trend is observed in the ACE variation than in the temperature effectiveness variation.

4.5. Thermal comfort analysis using PPD and PMV

Fig. 13 shows the density of PMV in the occupancy zone for the different scenarios. All the scenarios operating in the ventilation and heating mode met the PMV requirements for comfort category II. In ventilation mode, at least 50% of the occupancy zone in the scenarios S4, S8, and S12 and at least 75% of the occupancy zone in scenarios S3, S7, and S11 met the requirements for comfort category II. Furthermore, in scenario 5, at least 50% of the occupancy zone could even meet the requirement for comfort category I, and all twelve scenarios could satisfy the requirements for comfort category III.

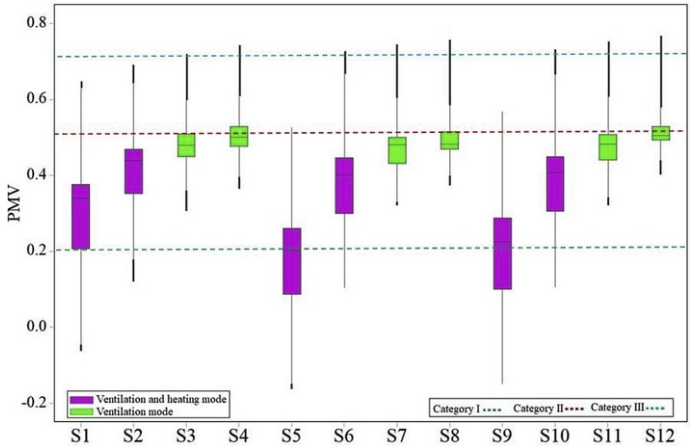

Fig. 13. Density of PMV in the occupancy zone.

alt-text: Fig. 13

The thick black lines in Fig. 13 represent outliers of the box plots which indicate some points in the convective plume of the occupant (above head level) with higher air temperature and velocity than the other parts of the occupancy zone.

The most interesting solutions from the point of view of energy use and IAQ can be seen in the scenarios where the AAH system ran at the minimum ventilation rate (S5–S8). The spatial distribution of the PPD for these scenarios is therefore illustrated in three different vertical cross sections in Fig. 14.

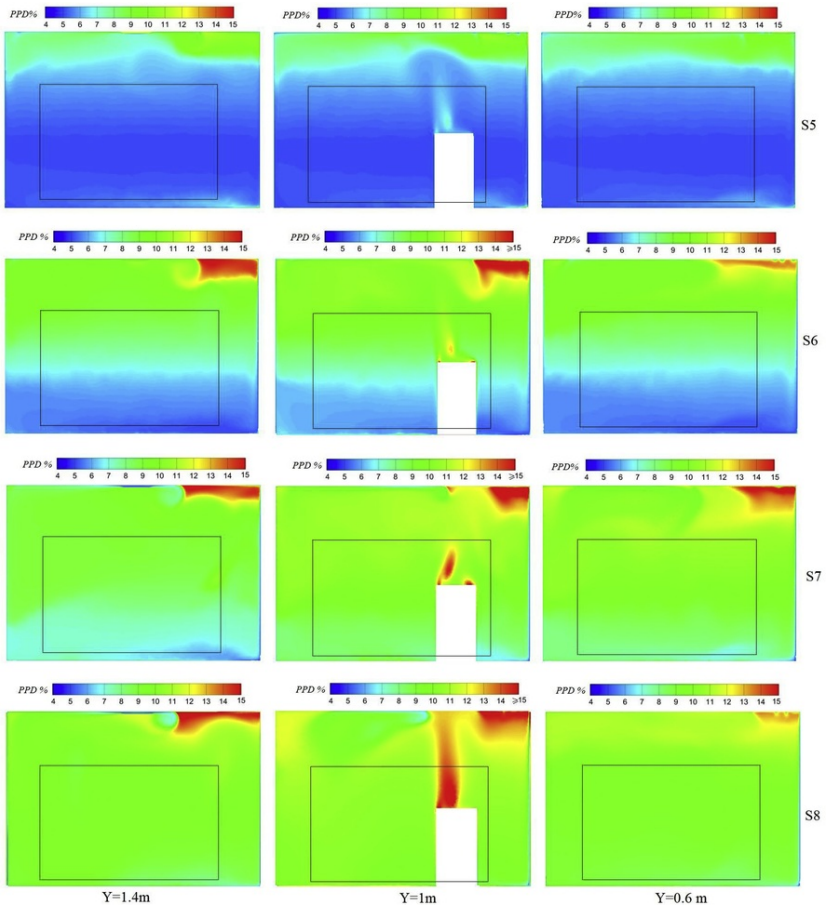

Fig. 14. Spatial variation in PPD for scenarios S5-S8 in the room. Note: the black rectangle represents the occupancy zone.

alt-text: Fig. 14

As Fig. 14 shows, all four scenarios roughly met the allowable dissatisfaction limit required for thermal comfort in the occupancy zone based on the standard EN ISO 7730 [15]. However, scenarios S5 and S6, in ventilation and heating mode, showed even lower PPD in the occupancy zone with the maximum around 6% and 8%, respectively, meeting the PPD requirements for thermal comfort category II [15].

Furthermore, if we take into account the relatively higher PPD values observed in some parts of the occupancy zone in scenarios S7 and S8, which have values for temperature effectiveness that are higher than 1 (see Fig. 12), this means that the supply temperature could be reduced to save energy use for space heating while still satisfying the thermal comfort requirements.

It is worth mentioning that the parameters PMV and PPD are static and that an adaptive thermal comfort analysis method or PMV test based on questionnaire responses from people surveyed would better represent the thermal comfort of occupants. However, it would not have been easy to perform these methods in this study, and the PMV and PPD indices are still good enough to illustrate system performance in terms of the thermal comfort of the occupant. The above-mentioned methods will be considered in future work.

5. Conclusions

This paper focused on the performance evaluation of the AAH system in an office cubicle equipped with a TTC-250 active supply diffuser and designed in accordance with the Norwegian PH standard requirements. Twelve scenarios based on the combination effect of various supply and outdoor conditions were analysed in terms of thermal comfort and IAQ indices, including both ventilation mode ($Ar > 0$) and ventilation and heating mode ($Ar < 0$). The

main findings revealed that:

- Applying the active supply diffuser with adjustable slot openings could avoid temperature stratification with a maximum temperature difference between 0.1 m and 1.1 m above the floor of around 1.5K, which met the recommended range for thermal comfort category II.
- The ADPI analysis showed that a supply of very negatively buoyant air can reduce the diffusion of air through the occupancy zone by as much as 75%. However, a relatively acceptable level of ACE and distribution of fresh supply air in the occupancy zone was achieved for all the scenarios, in contrast to previously implemented AAH systems not equipped with an active supply diffuser.
- PMV and PPD analysis indicated that using an active supply diffuser at least 50% of the occupancy zone in ventilation mode and 75% in ventilation and heating mode could satisfy the requirements for comfort category II, even when the active supply diffuser was operating at the minimum allowed ventilation rate.

Consequently, an AAH system equipped with an active supply diffuser could be considered as a viable low-temperature heating solution for space heating of office buildings with low energy use. Nevertheless, the performance of the active supply diffuser also needs to be investigated in the cooling season, since all-air systems use the same diffuser for both heating and cooling.

Acknowledgements

The authors would like to express their gratitude to Kari Thunshelle at SINTEF Building and Infrastructure for her contribution in providing technical information regarding the equipment functioning in the office cubicle.

Appendix

This appendix describes, the detailed equations associated with each index.

PMV and PPD

The expression for PMV is given by Eq. (13) as:

$$PMV = (0.303 \cdot \exp(-0.036.M) + 0.028) \cdot L \quad \textbf{(13)}$$

where M is the metabolic rate and L is the thermal load on the body expressed as Eq. (14) [15].

$$L = M - \frac{3.05}{1000} \cdot (5733 - 6.99 \cdot (M - W) - Pa) - 0.42 \cdot (M - W - 58.15) - \frac{1.7}{1000} \cdot (5867 - Pa) - 0.0014 \cdot M \cdot (34 - Ta) - 3.96 \cdot 10^{-8} \cdot Fcl \cdot \left((Tcl + 273)^4 - (Tr + 273)^4\right) - Fcl \cdot hc \cdot (Tcl - Ta) \quad \textbf{(14)}$$

where the clothing surface temperature (Tcl) is calculated as follows:

$$Tcl = 35.7 - 0.028 \cdot (M - W) - 0.155 \cdot Icl \cdot \left(3.96 \cdot 10^{-8} \cdot Fcl \cdot \left((Tcl + 273)^4 - (Tr + 273)^4\right) + Fcl \cdot hc \cdot (Tcl - Ta)\right) \quad \textbf{(15)}$$

PPD is then given as Eq. (16) [15]:

$$PPD = 100 - 95 \cdot \exp\left(-0.03353 \cdot PMV^4 - 0.2179 \cdot PMV^2\right) \quad \textbf{(16)}$$

ADPI

ASHRAE Standard 113 [17] states that the ADPI method should be applied for mixing systems under cooling only. Nevertheless, Liu and Novoselac [10] developed an EDT that can be applied in the ADPI method for heating applications like AAH, as defined in Eq. (17).

$$EDT = T_i - T_{ave.o} - 9.1 \cdot \left(v_i - 0.15\right) \quad \textbf{(17)}$$

where T_i (°C) is the local air temperature at point i, $T_{ave.o}$ (°C) is the spatial average air temperature in the occupancy zone, and v_i (m/s) is the local air velocity at point i. Overall, three criteria were applied for calculating ADPI in heating mode, given as follows [10]:

- EDT varying between −2.2 °C and 2 °C
- Local air velocity equal or less than 0.35 m/s

- Local maximum temperature difference between 0.1 m and 1.1 m less than 3K.

Therefore, the ADPI is determined as follows [2]:

$$\mathrm{ADPI} = \frac{\text{Number of test point that meet criteria}}{\text{Total number of test points}} \cdot 100\% \quad \textbf{(18)}$$

ACE

The ACE can be analysed in various ways. Age of air is a common method to calculate ACE. The local mean age of air indicates how long it takes for all the particles of fresh air to travel from the supply point to the point of study. It is an important index because if there is short-circuiting in the ventilation system, for example, the mean age of air would be high in the stagnant part of the room.

The mean age of air in the exhaust is called the nominal time constant τ_n .The average of all the local mean age of air (τ_i) values in the occupancy zone of the room gives the average age of air $< \overline{\tau} >$ in the occupancy zone. Thus, the local and average ACE of the room are defined by Eq. (19) [44] as:

$$\mathrm{ACE_i} = \frac{\tau_n}{2\,\tau_i} \cdot 100\ (\%), \quad \mathrm{ACE_{ave}} = \frac{\tau_n}{2 <\bar{\tau}>} \cdot 100\ (\%), \qquad \tau_n = \frac{V}{\dot{V}_s} \quad \textbf{(19)}$$

where V (m^3) is the room gross volume. The mean age of air in an ideal ventilation system in a fully mixed model (ACE = 50%) is the same throughout the room [19].

Temperature Effectiveness

This evaluates the temperature gradient in the space and is defined as follows:

$$\varepsilon_T = \frac{T_s - T_e}{T_s - T_{ave.o}} \quad \textbf{(20)}$$

where T_s (°C) is the supply air temperature, T_e (°C) is the exhaust air temperature.

References

[1] DIRECTIVE (EU), 2018/844 of the European parliament and of the council of 30 May 2018 amending Directive 2010/31/EU on the energy performance of buildings and Directive 2012/27/EU on energy efficiency (Text with EEA relevance), *Off. J. Eur. Union* 2018.

[2] N. Nord, Building energy efficiency in cold climates, *Encycl. Sustain. Technol.* 2017, 149–157.

[3] J.A. Myhren and S. Holmberg, Performance evaluation of ventilation radiators, *Appl. Therm. Eng.* **51** (1–2), 2013, 315–324.

[4] P.V. Nielsen, Lecture Notes on Mixing Ventilation Dept. Of Building Technology and Structural Engineering, 1995, Aalborg University U9513, 70.

[5] P.V. Nielsen, Velocity distribution in a room ventilated by displacement ventilation and wall-mounted air terminal devices, *Energy Build.* **31**, 2000, 179–187.

[6] K. Thunshelle, A. Cablé, M. Mysen and H.L. Hammer, Can air heating alone be used in passive house office building in cold climates? Review of the obtained results, In: *35th AIVC Conference, 4th TightVent Conference, 2nd Venticool Conference. , Poznan, Poland,* 2014.

[7] W.J. Fisk, D. Faulkner, D. Sullivan and F. Bauman, Air change effectiveness and pollutant removal efficiency during adverse mixing conditions, *Indoor Air* **7** (1), 1997, 55–63.

[8] F.J. Offermann and D. Int-Hout, Ventilation effectiveness measurements of three supply/return air configurations, *Environ. Int.* **15** (1), 1989, 585–592.

[9] A. Novoselac and J. Srebric, *Comparison of Air Exchange Efficiency and Contaminant Removal Effectiveness as IAQ Indices* **vol 109**, 2003, 339–349, (2).

[10] S. Liu and A. Novoselac, Air diffusion performance index (ADPI) of diffusers for heating mode, *Build. Environ.* **87**, 2015, 215–223.

[11] B.W. Olesen, A. Simone, M. Krajčík, F. Causone and M.D. Carli, Experimental study of air distribution and ventilation effectiveness in a room with a combination of different mechanical ventilation and heating/cooling

systems, *Int. J. Vent.* **9** (4), 2016, 371–383.

[12] M. Krajčík, A. Simone and B.W. Olesen, Air distribution and ventilation effectiveness in an occupied room heated by warm air, *Energy Build.* **55**, 2012, 94–101.

[13] D. Risberg, M. Vesterlund, L. Westerlund and J. Dahl, CFD simulation and evaluation of different heating systems installed in low energy building located in sub-arctic climate, *Build. Environ.* **89**, 2015, 160–169.

[14] A.Q. Ahmed, S. Gao and A.K. Kareem, Energy saving and indoor thermal comfort evaluation using a novel local exhaust ventilation system for office rooms, *Appl. Therm. Eng.* **110**, 2017, 821–834.

[15] NS-EN ISO 7730, Ergonomics of the Thermal Environment - Analytical Determination and Interpretation of Thermal Comfort Using Calculation of the PMV and PPD Indices and Local Thermal Comfort Criteria, 2006, Norwegian Standard; Norway.

[16] P.L. Miller and R.T. Nash, Further analysis of room air distribution performance, *ASHRAE Transact.* **77** (Pt 2), 1971, 205–212.

[17] ANSI/ASHRAE Standard 113, Method of Testing for Room Air Diffusion, 2009, American Society of Heating, Refrigerating and Air Conditioning Engineers; Atlanta, Georgia.

[18] ASHRAE, Handbook of Fundamentals, 2009, American Society of Heating, Refrigerating and Air Conditioning Engineers; Atlanta, Georgia.

[19] ANSI/ASHRAE 129-1997, Measuring Air-Change Effectiveness American Society of Heating, 2002, Refrigerating and Air- Conditioning Engineers.

[20] P.L. Miller and R.G. Nevins, Room air distribution with an air distributing ceiling—part II, *ASHRAE Transact.* **75**, 1969, 118–131.

[21] D.W. Etheridge and M. Sandberg, Building Ventilation: Theory and Measurement, 1996, John Wiley & Sons; Chichester, UK.

[22] P.V. Nielsen, *Lecture Notes on Mixing Ventilation* **U9513**, 1995, Aalborg: Dept. of Building Technology and Structural Engineering, Aalborg University Gul serie, (29).

[23] S.P. Corgnati, M. Perino, G.V. Fracastoro and P.V. Nielsen, Experimental and numerical analysis of air and radiant cooling systems in offices, *Build. Environ.* **44** (4), 2009, 801–806.

[24] S. Liu, J. Clark and A. Novoselac, Air diffusion performance index (ADPI) of overhead-air-distribution at low cooling loads, *Energy Build.* **134**, 2017, 271–284.

[25] P.L. Miller, Room air distribution performance of four selected outlets, *ASHRAE Transact.* **77** (2), 1971, 194–204.

[26] H. Amai and A. Novoselac, Experimental study on air change effectiveness in mixing ventilation, *Build. Environ.* **109**, 2016, 101–111.

[27] P.V. Nielsen, Fifty years of CFD for room air distribution, *Build. Environ.* **91**, 2015, 78–90.

[28] A. Cablé, M. Mysen and K. Thunshelle, Can Demand Controlled Ventilation Replace Space Heating in Office Buildings with Low Heating Demand?, 2014, Indoor Air conference; Hong Kong.

[29] TTC- Active Supply Diffuser, 2018, Available from: https://www.lindinvent.com/products/air-diffusers/ttc/, Accessed 4 May 2018.

[30] NS-3701-Criteria for Passive Houses and Low Energy Buildings, Non-residential Buildings, 2012, Norwegian Standard; Norway.

[31] STAR CCM+ Users Manual, 2017.

[32] L.M. Jiji, Heat Convection978-3-642-02971-4, 2 ed., 2009, Springer-Verlag Berlin Heidelberg.

[33] I.B. Celik, U. Ghia and P.J. Roache, Procedure for estimation and reporting of uncertainty due to discretization in CFD applications, *J. Fluids Eng.* **130**, 2008, 1–4.

[34] ANSI/ASHRAE Standard 62.1. Ventilation for Acceptable Indoor Air Quality, 2010, American Society of Heating, Refrigerating and Air-Conditioning Engineers; USA, Atlanta, GA.

[35] H.B. Awbi, Calculation of convective heat transfer coefficients of room surfaces for natural convection, *Energy Build.* **28** (2), 1998, 219–227.

[36] M.A.M. Brandan, Study of Airflow and Thermal Stratification in Naturally Ventilated Rooms, 2012, Department of Mechanical Engineering, Massachusetts Institute of Technology, Massachusetts Institute of Technology, 257

[37] H. Shahid and D. Naylor, Energy performance assessment of a window with a horizontal Venetian blind, *Energy Build.* **37** (8), 2005, 836–843.

[38] T. van Hooff, P.V. Nielsen and Y. Li, Computational fluid dynamics predictions of non-isothermal ventilation flow-How can the user factor be minimized?, *Indoor Air* **28** (6), 2018, 866–880.

[39] ANSI/ASHRAE/IESNA, Standard 90.1e2007 normative Appendix B: building envelope climate criteria, 2007.

[40] D. Int-Hout, Analysis of three perimeter heating systems by air-diffusion methods, *ASHRAE Transact.* **89** (Pt 1B), 1983, 101–112.

[41] ASHRAE, Thermal environmental conditions for human occupancy, ANSI/ASHRAE Standard 55e2010, 2010, American Society of Heating, Refrigerating and Air Conditioning Engineers; Atlanta, Georgia.

[42] P. Rohdin and B. Moshfegh, Numerical modelling of industrial indoor environments: a comparison between different turbulence models and supply systems supported by field measurements, *Build. Environ.* **46** (11), 2011, 2365–2374.

[43] K. Arendt and M. Krzaczek, Indoor Thermal Comfort Modeling and Simulation Using Computational Fluid Dynamics, 2016, Department of Building and Material Engineering, Faculty of Civil and Environmental Engineering, Gdańsk University of Technology.

[44] M. Mundt, H.M. Mathisen, M. Moser and P.V. Nielsen, Ventilation Effectiveness, 2004, REHVA Guidebooks.

Highlights

- Performance of an all-air heating system with active supply diffuser was studied.
- CFD analysis was done using different thermal comfort and air distribution indices.
- Archimedes number for various cases was defined to better interpret the results.
- Applying active supply diffuser could avoid strong temperature stratification.
- Minimum air diffusion performance index of 75% in the occupancy zone was reached.

Answer: W.J. Fisk, D. Faulkner, D. Sullivan and F. Bauman, Air change effectiveness and pollutant removal efficiency during adverse mixing conditions, Indoor Air, 7(1), 1997, 55–63.

Query: Please confirm that given names and surnames have been identified correctly and are presented in the desired order and please carefully verify the spelling of all authors' names.
Answer: I confirm that all given names and surnames provided in the proof are correct.

Query: Your article is registered as a regular item and is being processed for inclusion in a regular issue of the journal. If this is NOT correct and your article belongs to a Special Issue/Collection please contact n.antonyjc@elsevier.com immediately prior to returning your corrections.
Answer: I confirm that my article is registered as a regular item and is being processed for inclusion in a regular issue of the journal.